Construction and Building Materials 149 (2017) 327–337

Contents lists available at ScienceDirect

Construction and Building Materials

journal homepage: www.elsevier.com/locate/conbuildmat

Calibration and validation of a rutting model based on shear stress to strength ratio for asphalt pavements

Won Jae Kim, Van Phuc Le, Hyun Jong Lee *, Huy Thien Phan

Department of Civil and Environmental Engineering, Sejong University, South Korea

HIGHLIGHTS

- A rutting model in power law form was proposed.
- The model considers shear stress to strength ratio.
- Predictive equations for cohesion (c) and internal friction angle (ϕ) were developed.
- A rutting model was calibrated and validated using field rutting data.
- The model accurately estimate rut depths under varying load and environmental conditions.

ARTICLE INFO

Article history:
Received 23 February 2017
Received in revised form 2 May 2017
Accepted 6 May 2017

Keywords:
Rutting model
Shear stress
Shear strength
Asphalt pavement
Cohesion
Internal friction angle

ABSTRACT

In this study, a rutting model in power law form was proposed considering the shear stress to strength ratio which can be calculated in terms of cohesion (c) and internal friction angle (ϕ) for different asphalt mixtures. Predictive equations for c and ϕ were first developed from laboratory testing at a reference temperature of 50 °C using multiple regression analyses considering asphalt binder, aggregate and volumetric properties of different asphalt mixes. The predictive c and ϕ equations were found to have correlation coefficients of 0.87 and 0.86 respectively. The rutting model considers the number of load cycles (N), shear strength ratio, temperature and load duration as main parameters of the permanent strain wherein the coefficients were determined using tri-axial compressive strength and repeated load permanent deformation testing. It was calibrated using field rutting data from twenty-six Westrack pavement sections. Moreover, the rutting model was validated using field performance data obtained from Korean national highways' long term pavement performance database. It was found from the validation that the model can accurately estimate rut depths under varying load and environmental conditions in the fields.

1. Introduction

Permanent deformation is one of the major distresses occurring in asphalt concrete (AC) pavements. It typically manifests as rutting that appear as longitudinal depressions in the wheel paths accompanied by small upheavals to the sides. The rutting is highly dependent on the pavement structure, traffic and environment conditions. Since the rutting is a load-associated distress, the accurate prediction of rutting behavior of asphalt mixes plays an important role for asphalt pavement design and analysis. Therefore, a lot of research efforts have been made to develop rutting models that can accurately describe the rutting behavior of asphalt mixes.

Most of the available rutting models in the literature are empirical or mechanistic-empirical with limited fundamental material characterization. Thus, poor correlations with actual field performance are common results [1]. Recently more advanced rutting models [2–7] based on mechanics such as viscoelasticity, viscoelasticity and continuum damage approaches have been introduced. In general, these advanced models require much more sophisticated constitutive models for AC behavior that can describe its degradation response (e.g., the consequent permanent deformation, cracking, and other damages). As a result, the mechanistic models are rarely used in real practice in asphalt pavement design and analysis.

Permanent strain models [8–11] and permanent to resilient strain ratio models [12–16] are most well-known mechanistic empirical AC rutting models. Basic permanent strain models relate the permanent vertical strain to the number of load cycles and the extended version of the models explicitly consider the effects of temperature, induced stress level, and other parameters. Unlike the permanent strain models, the permanent to resilient strain ratio models consider the elastic response of pavement structure

* Corresponding author at: Department of Civil and Environmental Engineering, Sejong University, 98 Gunja-dong, Gwangjin-gu, Seoul 143-747, South Korea.
E-mail address: hlee@sejong.ac.kr (H.J. Lee).

http://dx.doi.org/10.1016/j.conbuildmat.2017.05.053
0950-0618/

through the resilient strain. Since the resilient strain governed by the stiffness of the pavement materials, stress level, layer thicknesses, temperature and others, all these effects are indirectly considered in the models.

Most of the permanent to resilient strain ratio models [13–16] do not explicitly consider the stress level and material parameters in the models because the resilient strain mostly takes care of those two effects. Although these models [13–16] are relatively simple to use, Archilla et al. [17] found that the AC dynamic modulus, which was one of the main material properties for calculating the resilient strain, was not a good parameter for describing the rutting behavior of asphalt mixes. Besides, these models are based on unconfined conditions, thus, they need an adjustment factor to consider the confinement effects in the models such as NCHRP 1-37A modeling approach.

Permanent deformation of AC layer is the result of a complex combination of densification and shear flow. The shear flow is a more dominant contributor to the permanent deformation occurred in the AC layer [18]. Therefore, some researchers [19,20] have tried to incorporate shear properties in the rutting models. One of the major significance of these models compared to the existing rutting models mentioned above is that a fundamental engineering property, shear strength, was incorporated into the models to represent the rutting resistance of the materials.

These two studies [19,20] gave great insights of the application of shear properties to the rutting prediction of asphalt mixes. However, it is limited since rutting tests were performed using wheel tracking machines which is incapable of providing an accurate simulation of field stress states. Moreover, the quantity of tests data is limited and field validation was not conducted.

A rutting model of asphalt mixes was established based on the shear stress to strength ratio in the authors' previous researches [21,22]. In the works, triaxial compressive strength (TCS) and repeated load permanent deformation (RLPD) tests on the three types of asphalt mixes with various volumetric properties were performed at multiple load levels and temperatures to correlate shear properties to rutting performance. The model coefficients were independent of mix types and loading magnitudes. The model could successfully predict the permanent deformation of various mixes all the way up to the tertiary flow with a high level of prediction accuracy. The model was also calibrated using accelerated performance testing (APT) data.

Although the authors' original rutting model [22] showed some advantages compared to the existing mechanistic-empirical rutting models, one of the major weakness is that the model needs more tests efforts to characterize shear properties of asphalt mixes. In addition, the model requires calibration and validation with various rutting performance data obtained from fields.

Therefore, the main objectives of this study are to develop prediction equations for shear properties of asphalt mixes and to calibrate and validate the rutting model. To accomplish these objectives, additional laboratory tests were first conducted to measure shear properties of various asphalt mixes with different volumetric properties and testing conditions. The prediction equations for cohesion and friction angle were developed using the tests data and the rutting model form was revised. Finally, the rutting model was calibrated with WesTrack data [23] and validated with field performance data obtained in Korea.

2. Review of previous model

In the authors' previous research [21,22], a rutting model based on shear stress to strength ratio was developed using the TCS and RLPD tests results conducted on three types of asphalt mixes (i.e., two dense-graded mixes of maximum aggregate size of 19 mm with PG64-22 and PG76-22 asphalt binders, respectively and Stone Mastic Asphalt (SMA) with PG64-22 asphalt binder) under three different combinations of deviatoric stresses and confining pressures, and three temperature conditions. Additionally, the effects of loading frequencies were evaluated at four load durations (i.e., 0.1, 0.2, 0.4, and 0.8 s). In the previous studies, RLPD test results revealed an excellent exponential correlation between shear stress to strength ratio $\frac{\tau}{\tau_f}$ and permanent strain ϵ_p under certain load repetitions [21]. From laboratory test data, a rutting model based on shear stress to strength ratio was proposed:

$$\varepsilon_p = 2.9895 \times 10^{-3} e^{6.2807\times10^{-6}N} e^{3.6723\frac{\tau}{\tau_f}N^{0.1032}} t^{0.4224} \quad (1)$$

such that

$R^2 = 0.946$,
root mean square error = 0.006, and
average error = 13.34%.

In Eq. (1), N and t are number of load cycles and load duration, respectively. The shear stress to strength ratio can be calculated as follows:

$$\frac{\tau}{\tau_f} = \frac{(\sigma_1 - \sigma_3)(\tan\phi \sin\phi + \cos\phi - \tan\phi)}{2(c + \sigma_3 \tan\phi)} \quad (2)$$

where

ε_p = permanent strain,
τ = shear stress (kPa),
τ_f = shear strength (kPa),
N = number of load cycles,
t = load duration of each cycles (second),
σ_1 = actual major principle stress under the given loading condition (kPa),
σ_3 = actual minor principle stress under the given loading condition (kPa),
c = cohesion (kPa), and
ϕ = friction angle (°).

In addition to the rutting model, the authors proposed the prediction equations for the cohesion and friction angle as follows:

$$c = \alpha_0 + \alpha_1 T + \alpha_2 AC + \alpha_3 AV \quad (3)$$

$$\phi = \beta_0 + \beta_1 T + \beta_2 AC + \beta_3 AV \quad (4)$$

where

AC = binder content (%),
AV = air-void content (%),
T = temperature (°C), and
α_i and β_i = regression coefficients are based on asphalt mixtures.

The prediction equations of the cohesion and friction angle in Eqs. (3) and (4), respectively, are not useful for practical purposes because material coefficients α_i and β_i change when asphalt mix properties change. Therefore, new prediction equations for the cohesion and friction angle were proposed in this study.

3. Experimental program

3.1. Materials and specimen preparation

As mentioned earlier, the TCS tests were conducted on three asphalt mixes to obtain shear properties in the previous study [21,22]. In this study, laboratory tests were performed on four additional types of asphalt mixes with various air voids and binder contents. Information on the seven mixes including the three mixes obtained from the previous study is provided in Table 1.

Table 1
Mix properties.

Mix Type	Binder Grade	Mix ID	Asphalt Content (%)	Air Void (%)	VMA (%)	VFA (%)
A	PG64-22	A-4.0	4.0	7.2	14.3	49.7
		A-4.5	4.5	4.8	13.2	63.7
		A-5.0	5.0	2.8	12.5	77.7
		A-5.5	5.5	1.7	12.7	86.6
		A-6.0	6.0	1.3	13.4	90.3
B	PG76-22	B-4.0	4.0	7.7	16.2	52.4
		B-4.5	4.5	5.7	15.5	63.1
		B-5.0	5.0	3.2	14.3	77.7
		B-5.5	5.5	2.1	14.1	85.1
		B-6.0	6.0	1.8	15.3	88.2
C	PG64-22	C-5.0	5.0	7.2	20.7	65.3
		C-5.5	5.5	5.5	20.3	72.9
		C-6.0	6.0	4.2	20.2	79.3
		C-6.5	6.5	2.8	20.1	86.1
		C-7.0	7.0	2.1	20.6	89.6
D	PG58-22	D-4.5	4.5	4.7	14.1	66.8
		D-5.0	5.0	2.7	13.3	79.6
		D-5.5	5.5	0.6	13.2	95.1
		D-6.0	6.0	0.2	13.6	99.2
E	PG64-22	E-4.5	4.5	6.5	18.2	64.2
		E-5.0	5.0	4.4	17.5	74.8
		E-5.5	5.5	2.9	17.0	82.8
		E-6.0	6.0	1.2	17.3	92.9
F	PG64-22	F-4.5	4.5	6.5	11.6	31.2
		F-5.0	5.0	5.6	11.1	49.5
		F-5.5	5.5	2.5	9.6	74.1
		F-6.0	6.0	2.5	10.7	76.8
G	PG64-22	G-4.5	4.5	7.6	13.0	41.5
		G-5.0	5.0	5.8	12.2	52.3
		G-5.5	5.5	3.5	12.1	71.5
		G-6.0	6.0	2.0	11.2	81.9

Note:
1. Data for the Mixes A, B and C are obtained from the previous studies [21,22]
2. A,B, and D are 19 mm dense grade; E is 25 mm dense grade; F is 13 mm fine grade; G is 13 mm fine plus grade; C is 13 mm stone mastic asphalt (SMA); VMA = voids in mineral aggregate; VFA = voids filled with asphalt.

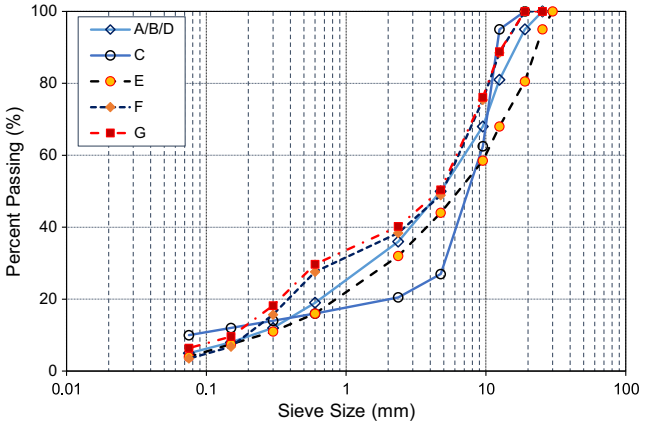

Fig. 1. Aggregate gradations.

Aggregate gradations used for the seven mixes are also presented in Fig. 1.

Instead of the TCS tests, Christensen and Bonaquist [24] proposed a simplified method for determining shear properties c and ϕ based on indirect tensile (IDT) and uniaxial compressive strength (UCS) tests. This simplified method was validated by Li et al. [22]. For the simplicity of testing, the IDT and UCS tests were adopted in this study to measure shear properties.

A Superpave gyratory compactor was used to produce specimens with the diameter of 150 mm and the height of 175 mm. The gyratory compacted specimens were then cored and sawed to obtain the required 100 mm diameter by 150 mm tall specimens for the UCS testing. In addition, the compacted specimens were cut into two parts to obtain the required 50 mm high specimens for the IDT testing.

3.2. Testing methods

The UCS and IDT tests were performed at a displacement rate of 50 mm/min under three temperature conditions of 40, 50, and 60 °C using a servo-hydraulic testing system. The peak compressive load was measured to calculate the strength of all the specimens.

4. Test results

Christensen and Bonaquist [24] proposed a simple method for determining cohesion and friction angle based on the IDT and UCS test data using following equations:

$$\tan\alpha = \frac{|\sigma_{UCS}| - 4|\sigma_{IDT}|}{|\sigma_{UCS}| - 2|\sigma_{IDT}|} \tag{5}$$

$$\phi = \sin^{-1}(\tan\alpha) \tag{6}$$

$$c = \left(\frac{2 - \tan\alpha}{\cos\phi}\right)\sigma_{IDT} \tag{7}$$

where $\tan\alpha$ = slope parameter,
σ_{IDT} = indirect tensile strength, and
σ_{UCS} = uniaxial compressive strength.

The cohesion and friction angle values for all the specimens were calculated using Eqs. (5)(7) with the uniaxial compressive and indirect tensile strengths data obtained from the laboratory tests and summarized in Table 2.

Table 2
Summary of test results.

Mix Type	Mix ID	T (°C)	σ_{UCS} (kPa)	σ_{IDT} (kPa)	c (kPa)	ϕ (°)
A	A-5.0	40	–	–	587	44
	A-4.0	50	–	–	367	47
	A-4.5	50	–	–	377	43
	A-5.0	50	–	–	378	42
	A-5.5	50	–	–	376	41
	A-6.0	50	–	–	353	42
	A-5.0	60	–	–	250	39
B	B-5.0	40	–	–	847	43
	B-4.0	50	–	–	558	48
	B-4.5	50	–	–	626	41
	B-5.0	50	–	–	624	39
	B-5.5	50	–	–	611	39
	B-6.0	50	–	–	573	38
	B-5.0	60	–	–	472	37
C	C-6.5	40	–	–	521	48
	C-5.0	50	–	–	367	48
	C-5.5	50	–	–	381	47
	C-6.0	50	–	–	367	47
	C-6.5	50	–	–	348	46
	C-7.0	50	–	–	326	45
	C-6.5	60	–	–	254	42
D	D-5.0	40	2531	234	452	51
	D-4.5	50	1416	143	269	48
	D-5.0	50	1307	160	287	46
	D-5.5	50	1198	127	236	47
	D-6.0	50	1145	124	229	46
	D-5.0	60	1053	101	160	44
E	E-5.0	40	1717	225	398	40
	E-4.5	50	1310	132	240	44
	E-5.0	50	1341	153	280	45
	E-5.5	50	1184	111	214	50
	E-6.0	50	1080	110	207	48
	E-5.0	60	902	89	169	49
F	F-5.0	40	2410	285	516	44
	F-4.5	50	1810	163	318	51
	F-5.0	50	2573	329	586	41
	F-5.5	50	1907	246	347	41
	F-6.0	50	1759	209	378	44
	F-5.0	60	1159	84	177	56
G	G-5.5	40	2762	315	575	45
	G-4.5	50	1599	178	326	46
	G-5.0	50	1676	314	380	41
	G-5.5	50	1450	182	325	42
	G-6.0	50	1351	187	329	38
	G-5.5	60	1053	101	182	46

Note: Data for the Mixes A, B and C are obtained from the previous studies [21,22].

5. Development of AC rutting model

The authors' original rutting model in Eq. (1) implicitly considers the temperature effects through the tensile strength as shown in Eqs. (3) and (4). Since both the shear strength and stress are influenced by temperature, the effects of temperature may need to be considered explicitly.

To evaluate the temperature effects to the shear strength, the c and ϕ values at varying temperatures were compared for all the asphalt mixes as shown in Figs. 2 and 3. As seen in Fig.2, the cohesion and temperature has a power form relationship in general. Meanwhile, the relation of friction angle and temperature does not show any significant trend as shown in Fig.3. Therefore, it was decided to consider the temperature effects explicitly in the rutting model.

Before developing a rutting model, the prediction equations for the cohesion and friction angle were first developed. There are various material properties affecting the cohesion and friction angle. They are physical properties of asphalt binder and aggregate and volumetric properties of asphalt mixes.

Using the experimental data in Table 2, a series of multiple regression analyses were performed to determine the relations of shear properties to the material properties of asphalt mixes. After the regression analysis, the final forms of the prediction equations for the cohesion and friction angle established are as follows:

$$c_{ref} = a_0 + a_1 AC + a_2 VMA + a_3 VFA + a_4 P_{200} + a_5 \frac{G^*_{ref}}{\sin \delta_{ref}} + a_6 \log(\delta_{ref}) + a_7 AC^2 + a_8 P_{200}^2 + a_9 VMA \times P_{200} \quad (R^2 = 0.87) \tag{8}$$

$$\phi_{ref} = b_0 + b_1 AC + b_2 VMA + b_3 \rho_4 + b_4 P_{200} + b_5 \log(\delta_{ref}) + b_6 \log^2(\delta_{ref}) + b_7 \frac{VFA}{VMA} + b_8 VFA + b_9 P_{200}^2 + b_{10} \rho_4^2 + b_{11} VMA P_{200} + b_{12} \rho_4 \times VMA \quad (R^2 = 0.86) \tag{9}$$

where

AC = binder content (%),
VMA = voids in mineral aggregate (%),
VFA = voids filled with asphalt (%),
ρ_4 = percent cumulative retained on 4.75 mm sieve (%),
P_{200} = percent passing on the 0.075 mm sieve (%),
G^*_{ref} = binder stiffness at reference temperature of 50 °C (kPa),

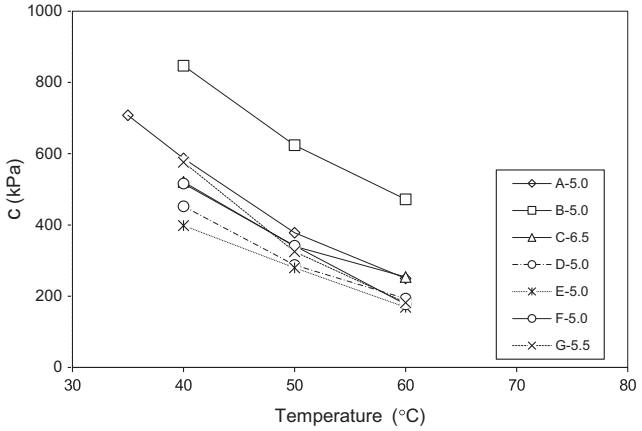

Fig. 2. Relationship between c value and temperature.

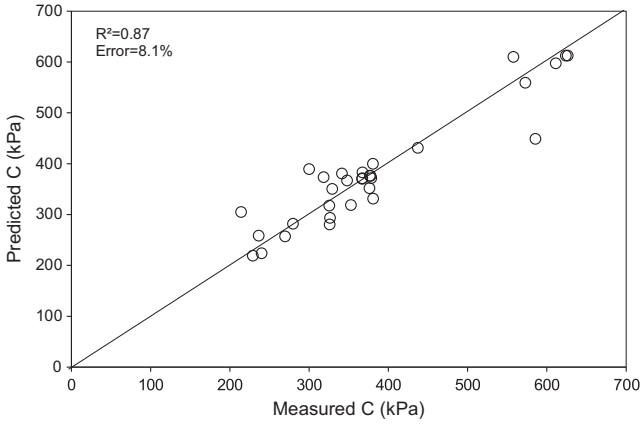

Fig. 4. Comparison of measured and predicted c value.

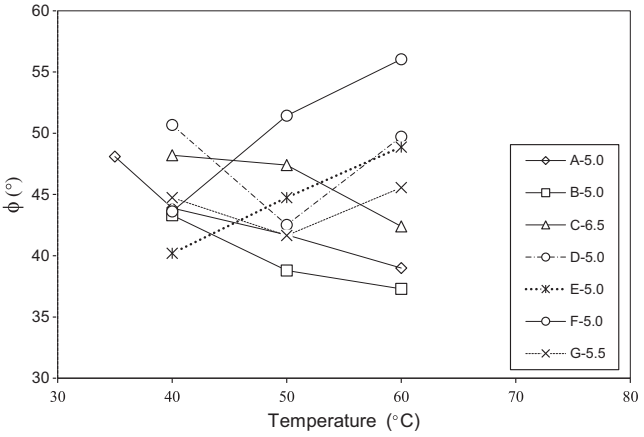

Fig. 3. Relationship between ϕ value and temperature.

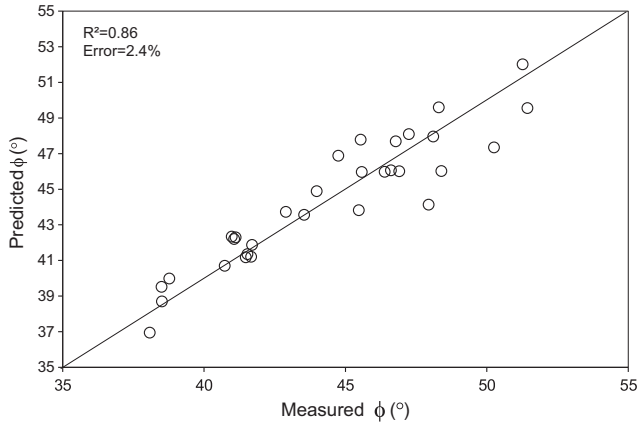

Fig. 5. Comparison of measured and predicted ϕ value.

δ_{ref} = binder phase angle at reference temperature of 50 °C (degrees), and

a_0, a_1,. . ., a_9, b_0, b_1, . . ., b_{12} = regression coefficients provided in Table 3.

It is noted here that the prediction equations for c and ϕ in Eqs. (8) and (9) are only valid at the reference temperature of 50 °C.

Figs. 4 and 5 respectively show comparisons between the measured and predicted c and ϕ values using Eqs. (8) and (9). It is observed that the predicted values are in a good agreement with the experimental results. The correlation coefficients between the measured and predicted values are 0.87 and 0.86 for c and ϕ values, respectively.

Table 3
Regression coefficients of Eqs. (8) and (9).

C		ϕ	
a_0	9534.656	b_0	635865.271
a_1	96.450	b_1	−2.109
a_2	31.537	b_2	25.003
a_3	−0.052	b_3	−234.014
a_4	−225.653	b_4	210.598
a_5	−12.655	b_5	−668404.905
a_6	−4526.946	b_6	177161.697
a_7	−12.606	b_7	−0.528
a_8	41.113	b_8	0.058
a_9	−14.267	b_9	−23.345
		b_{10}	2.190
		b_{11}	0.487
		b_{12}	−0.504

The authors' original rutting model in Eq. (1) has an exponential form and is not easy to handle mathematically. For example, the number of load cycles to certain plastic strain level is difficult to be directly determined from Eq. (1). Since the power law models [13–16,19,25] has been widely used to describe the relation between the cumulative permanent strain and the number of load cycles [13–16,19,25], it is decided to revise the authors' original rutting model by applying a power law model.

An analysis of variance (ANOVA) was applied to evaluate the effect of load cycles N, shear stress to strength ratio $\frac{\tau}{\tau_f}$, temperature T, and load duration t on measured plastic strain. Based on the ANOVA testing as shown in Table 4, they have a significant influence with the measured plastic strain at 5% level of significance.

Letting the number of load cycles N, shear stress to strength ratio $\frac{\tau}{\tau_f}$, temperature T, and load duration t as major governing parameters for the permanent strain ε_p, the following power form for the rutting model was assumed:

$$\varepsilon_p = k_0(N)^{k_1}\left(\frac{\tau}{\tau_f}\right)^{k_2}_{ref}(T)^{k_3}(t)^{k_4} \quad (10)$$

where k_i are model coefficients and $(\tau/\tau_f)_{ref}$ is ratio of shear stress at an arbitrary temperature to shear strength at a reference temperature of 50 °C under the same confining pressure. The $(\tau/\tau_f)_{ref}$ can be calculated as follows:

Table 4
Results of ANOVA on Main Effects on rutting model.

Source	Sum of squares	df	Mean square	F	p-Value	Significant
Load cycles (N)	0.02224972	7	0.003179	7.583443	<0.001	Yes
Strength ratio (τ/τ_f)	0.023917	23	0.00104	2.35448	<0.001	Yes
Temperature (T)	0.016528	2	0.008264	26.385	<0.001	Yes
Load duration (t)	0.008313	3	0.002771	7.640361	<0.001	Yes

$$\left(\frac{\tau}{\tau_f}\right)_{ref} = \frac{\tau_{max}(\tan\phi_{ref}\sin\phi_{ref} + \cos\phi_{ref} - \tan\phi_{ref})}{c_{ref} + \sigma_3\tan\phi_{ref}} \quad (11)$$

where

τ_{max} = maximum shear stress under the given loading condition,

σ_3 = actual minor principle stress under the given loading condition,

c_{ref} = cohesion at reference temperature of 50 °C (kPa), and

ϕ_{ref} = friction angle at reference temperature of 50 °C (°).

After the statistical analysis of the TCS and RLPD tests data obtained from the previous study [21,22], the coefficients of Eq. (10) were determined and are as follows:

$$\varepsilon_p = 10^{-15.0247}(N)^{0.29425}\left(\frac{\tau}{\tau_f}\right)_{ref}^{2.7844}(T)^{6.79174}(t)^{0.44878} \quad (12)$$

To verify the rutting model proposed in Eq. (12), permanent strain values were calculated using Eq. (12) with Eqs. (8) and (9) and compared with the measured values from the RLPD tests. Fig. 6 shows a comparison between measured and predicted permanent strains. It is observed in the figure that the predicted values are in a good agreement with the experimental results. The correlation coefficient between the measured and predicted strains is 0.94 and has an average root mean square error (RMSE) of 0.008. This implies that the proposed rutting and shear properties models successfully predicted the rutting behavior of various asphalt mixes.

6. Calibration

Although the AC rutting model proposed in this study successfully predicted the permanent strain values measured in the laboratory tests for various asphalt mixes, the model should be calibrated using field data because of the difference in loading and environmental conditions between the field and laboratory. Thus, the prediction equation for the rutting model was calibrated using the field rutting data obtained from the 26 pavement sections of WesTrack testing [23].

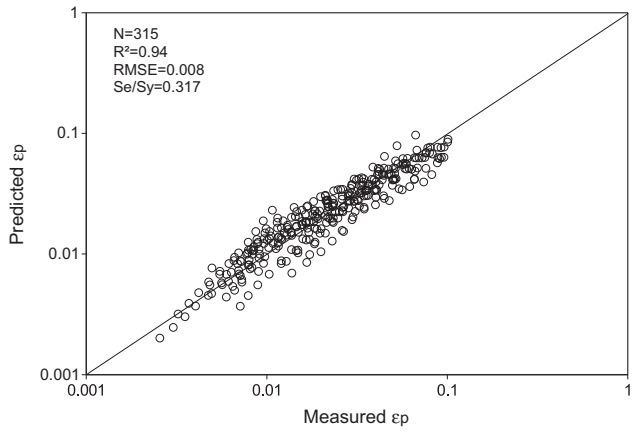

Fig. 6. Comparison of measured and predicted permanent strains.

In order to calibrate the rutting model, calibration coefficients were assigned in Eq. (12) as follows:

$$\varepsilon_p = 10^{-15.0247\alpha_0}(N)^{0.29425\alpha_1}\left(\frac{\tau}{\tau_f}\right)_{ref}^{2.7844\alpha_2}(T)^{6.79174\alpha_3}(t)^{0.44878\alpha_4} \quad (13)$$

where α_i is calibration coefficients for the rutting models.

In the WesTrack testing [23], all the pavement sections have the same thickness as shown in Fig. 7 but materials of AC layer and subgrade are different. For the AC layer, PG64-22 asphalt binder and three different aggregate gradations were used. The loading conditions were maintained constant for all the time. Incremental cumulative permanent strain was calculated for every hour to account for the effects of temperature change with time. To accurately compute the rut depth, the AC layer was divided into three sublayers as seen in the same figure.

The AC dynamic modulus of each sublayer was predicted based on its volumetric properties, gradation, specific temperature, and frequency using Hirsch model [26] which was validated in the previous work [27]. Resilient moduli of 138 MPa for the aggregate subbase of all the sections and various modulus values for subgrade provided in the report [23] were used. Poisson's ratio values of 0.35, 0.4 and 0.45 were assumed for asphalt layer, aggregate subbase and subgrade, respectively [23].

Since temperature data only at the pavement surface was available in the report [23], temperatures of the AC pavement at various depths were predicted using Bells equation [28] with coefficients proposed by Lukanen et al. [29] as follows:

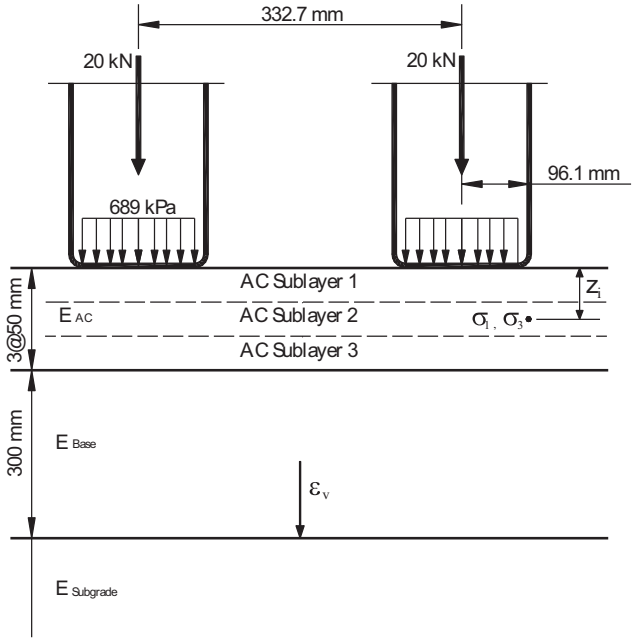

Fig. 7. WesTrack pavement representation for calibration of rutting model.

$$T_d = 2.8 + 0.894 \times IR + \{\log(d) - 1.5\} \times \{-0.54 \times IR + 0.77 \times (5 - day) + 3.763 \times \sin(hr - 18)\} + \{\sin(hr - 14)\} \times \{0.474 + 0.031 \times IR\} \quad (14)$$

where

T_d = pavement temperature at depth d (°C),
IR = surface temperature (°C),
d = depth (mm) at which pavement temperature is predicted,
5-day = mean air temperature, (°C) during the previous 5 days, and
hr = time of day in 24-h system.

The loading time at effective depth in AC layers was estimated by the following equation proposed in NCHRP [15]:

$$t = \frac{2 \times (a + d_{eff})}{277.8 \times V} \quad (15)$$

where

t = loading time (s),
a = tire contact radius (mm),
d_{eff} = effective depth (mm), and
V = vehicle speed (km/h).

KENLAYER, a multilayered elastic program, was used to calculate the principal stresses (σ_1 and σ_3) in AC sublayers and vertical compressive strain (ε_v) on the top of the subgrade surface. Since the incremental permanent strain for every hour was to be calculated, the structural analysis should be performed for every hour which requires a lot of analysis time. Thus, to save analysis time, a series of regression analysis was conducted to determine the principal stresses and vertical strains at any temperature within each pavement section such as Fig. 8. Regression equations were then used to determine stress and strain values for various temperature conditions.

The c and ϕ values of each AC sublayer were determined based on the binder contents, volumetric properties, and gradations for the 26 pavement sections using Eqs. (8) and (9). Eq. (11) was used to calculate the shear stress to strength ratio value for each sublayer. The permanent strain value for each sublayer was estimated using Eq. (12) for a given number of load cycles and temperature.

The time–hardening scheme [1] is used to determine the cumulative permanent strains occurred in AC sublayers for the i^{th} time interval as follows:

$$\varepsilon_{p,1} = a_1[\Delta N_1]^{k_1} \quad (16)$$

$$\varepsilon_{p,t} = a_t\left[\left(\frac{\varepsilon_{p,t-1}}{a_t}\right)^{\frac{1}{k_1}} + \Delta N_t\right]^{k_1} \quad (17)$$

where

$a_t = k_0\left(\frac{\tau}{\tau_{f,t}}\right)^{k_2}_{ref}(T)^{k_3}(t)^{k_4}$,
τ_{f_t} = shear strength for the t^{th} hour of loading,
$\varepsilon_{p,t}$ = permanent strain for the t^{th} hour of loading, and
ΔN_t = number of load application during the t^{th} hour.

Similarly, the time–hardening scheme was used to compute the rut depth of unbound layers. The equation used to calculate rut depth for unbound material in this study is as follows [30]:

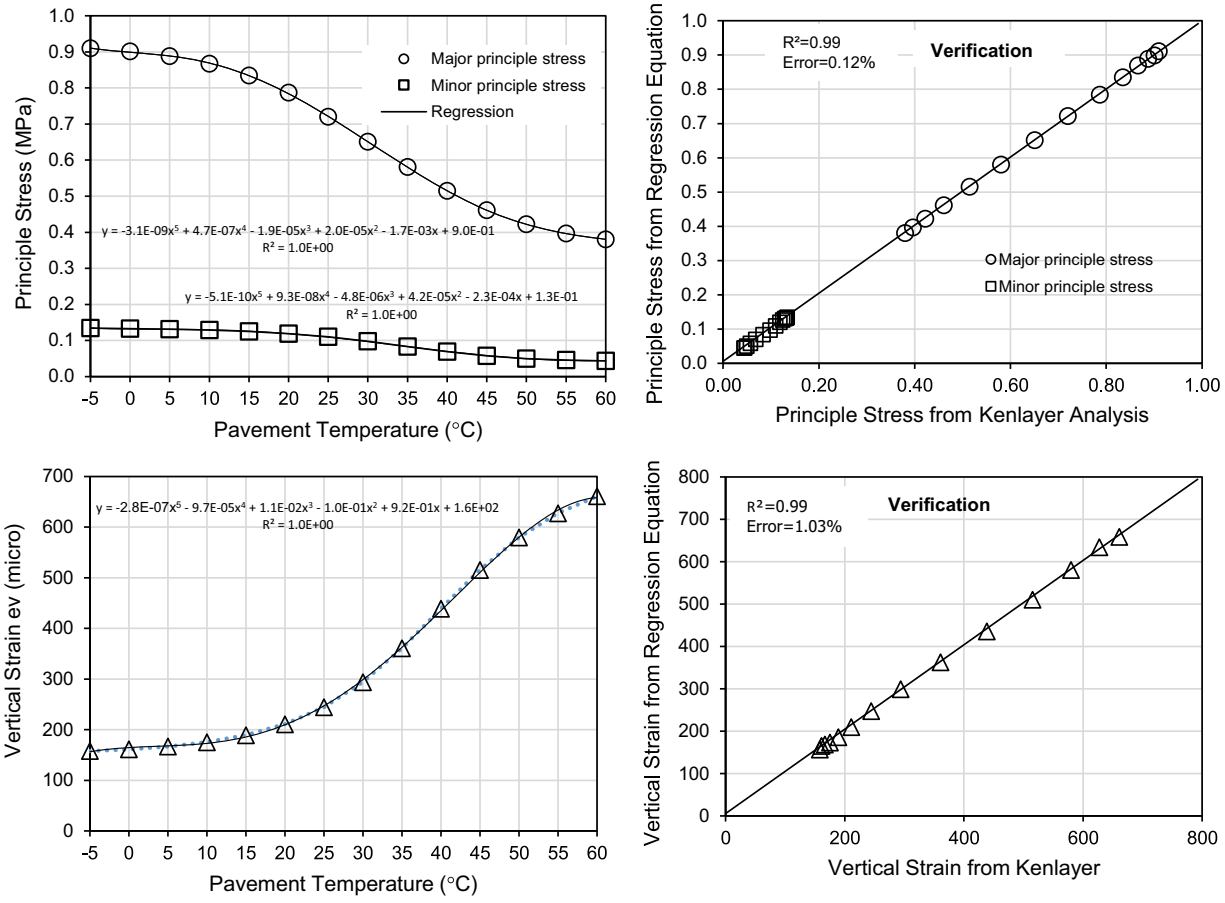

Fig. 8. Typical relation between principle stresses and vertical strain versus temperature.

$$rd_t = d_t\left[\left(\frac{rd_{t-1}}{d_t}\right)^{\frac{1}{0.372}} + \Delta N_t\right]^{0.372} \quad (18)$$

where

$$d_t = \frac{3.548}{[1.05\times 10^{-9}\varepsilon_{v,t}^{-4.484}]} \text{ and} \quad (19)$$

$\varepsilon_{v,t}$ = vertical compressive strain at surface of subgrade for the tth hour of loading.

The overall rut depth is computed as the sum of rut depth of individual sublayers that is obtained by multiplying the calculated permanent strain by the thickness of each layer and rut depth occurred in unbound layers:

$$RD = \sum_{i=1}^{n}\varepsilon_{pi}h_i + rd \quad (20)$$

where

RD = total rut depth,
n = number of sublayers,
ε_{pi} = permanent strain in sublayer i,
h_i = thickness of sublayer i, and
rd = rut depth of unbound material.

Using the procedure mentioned above, a trial and error approach was conducted to determine the calibration coefficients of the rutting models in Eq. (13). The predicted rut depth and measured one were compared using an error minimization technique. As a result, the calibration coefficient α_0 was found to be 0.955 and all other coefficients were 1.0.

Fig. 9 shows typical comparison results between the predicted and measured rut depth for sections 1 (fine), 7 (coarse), 24 (coarse) and 19 (fine-plus) in WesTrack [23]. It can be seen from the figure that the predicted rut depths generally fit well with the measured ones.

To evaluate the prediction error of the proposed rutting model, the predicted and measured rut depths for all the sections were compared in Fig. 10. As seen in the figure, the correlation coefficient is 0.96 and the average root mean square error (RMSE) is 2.35 mm.

7. Validation

Independent field rutting performance data obtained from Long Term Pavement Performance (LTPP) in Korea were used to validate the calibrated rutting model. The LTPP data were collected from 8 different road sections of national highways located in various

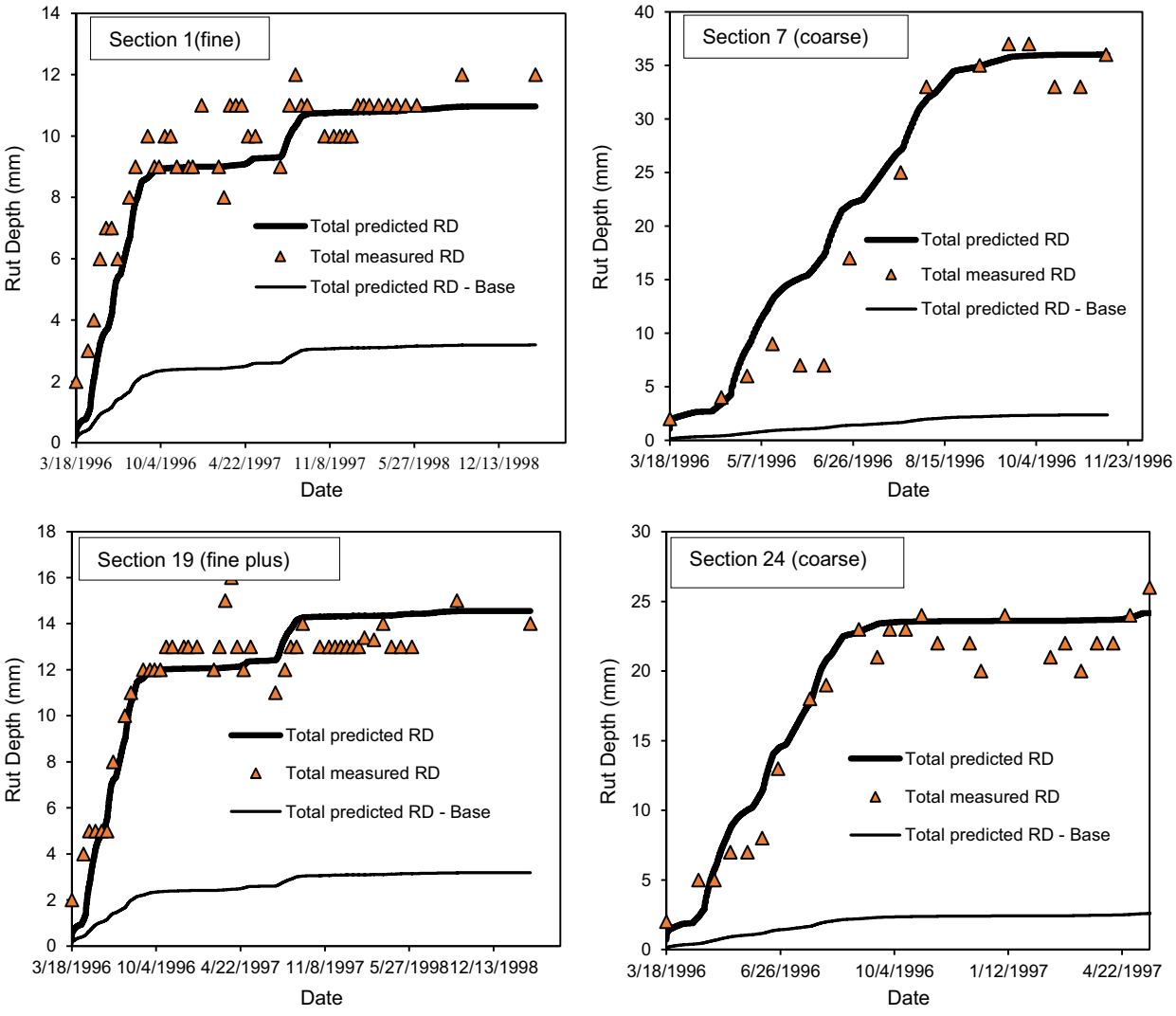

Fig. 9. Typical comparison results between predicted and measured rut depths with time.

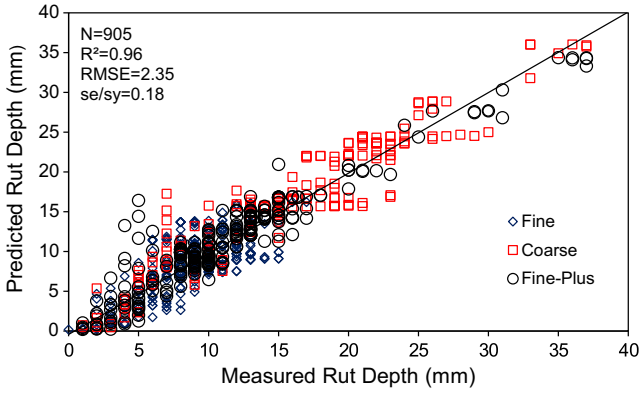

Fig. 10. Comparision of measured and predicted rut depth for 26 sections.

areas as shown in Table 5. The vehicle speed used in this analysis is 60 km/h. The resilient modulus of subgrade and subbase were estimated from the back-calculation of FWD test data conducted right after the construction of each section. Adjusting the moduli values for AC and unbound material is controlled until the error of the back-calculated modulus is less than 5% [31] and are provided in Table 6. The AC dynamic modulus of each section was predicted from Hirsch model using volumetric properties in Table 7, gradation, specific temperature, and frequency. The Poisson's ratios of asphalt layer, subbase and subgrade were assumed to be 0.35, 0.4 and 0.45, respectively. And temperatures of the AC pavement at various depths were predicted using Eq. (14).

Following the same procedure used in the calibration, rut depth values for all the LTPP sections were estimated and compared with measured values. Some comparison results between the predicted and measured rut depth development are shown in Fig. 11. Overall, the predicted rut depth matches well with the measured rut depth in the field.

To evaluate the prediction accuracy of the rutting model, the predicted and measured rut depth values for all the sections were compared in Fig. 12. The correlation coefficient R^2 is 0.87 and the average root mean square error (RMSE) is 1.19 mm, which indicates that the calibrated rutting prediction model was able to accurately predict field rut depth under varying load and environmental conditions.

Table 5
Traffic information of LTPP sections.

Sections	Highway Route No.	Construction Date	ESAL							
			2006	2007	2008	2009	2010	2011	2012	2013
L1	46	Dec. 2005	185,891	284,319	151,824	311,226	178,461	482,549	630,322	460,968
L2	44	Nov. 2006	1,005,652	931,922	673,755	914,767	1,403,989	1,158,026	1,849,533	1,739,154
L3	21	Jan. 2008	–	–	531,832	822,755	748,875	3,331,004	2,808,393	2,706,895
L4	23	Dec. 2005	672,831	629,901	1,327,814	1,233,969	1,308,487	1,748,576	1,625,640	1,620,716
L5	18	Jan. 2008	–	–	517,845	466,784	549,973	793,639	834,656	617,333
L6	17	Jan. 2008	–	–	2,212,656	2,053,381	2,021,917	2,222,066	2,634,736	3,391,617
L7	77/82	Jan. 2008	–	–	632,811	1,232,212	1,670,265	2,285,540	925,859	2,072,461
L8	1	Jan. 2008	–	–	701,648	725,976	835,163	1,030,823	1,107,091	1,681,702

Table 6
Structure and resilient modulus of unbound material of LTPP sections.

Sections	Layer Thickness (cm)				Resilent Modulus (MPa)	
	AC Surface	AC Binder	AC Base	Subbase	Subbase	Subgrade
L1	6.0	–	20.0	30.0	346	121
L2	6.0	6.0	14.0	30.0	116	119
L3	5.0	6.0	19.0	20.0	220	129
L4	5.0	6.0	15.0	34.0	146	106
L5	5.0	–	20.0	35.0	60	74
L6	5.0	6.0	21.0	36.0	191	221
L7	5.0	7.0	20.0	20.0	116	81
L8	5.0	6.0	16.0	30.0	89	50

Table 7
Asphalt mix properties of LTPP sections.

Sections	Binder Content (%)			VMA (%)			VFA(%)		
	AC Surface	AC Binder	AC Base	AC Surface	AC Binder	AC Base	AC Surface	AC Binder	AC Base
L1	6.8	–	4.0	23.1	–	18.2	75.3	–	58.3
L2	6.3	5.0	4.0	19.0	15.2	18.1	68.4	68.4	58.5
L3	5.0	4.8	4.0	14.8	17.8	18.6	70.9	54.0	56.5
L4	5.4	4.8	3.7	17.8	16.2	16.4	61.9	60.5	61.5
L5	5.5	–	4.2	19.2	–	19.3	57.8	–	56.5
L6	5.4	5.0	4.1	17.8	14.6	17.4	61.5	71.9	63.1
L7	5.2	5.0	4.0	17.8	16.4	18.4	59.5	62.7	56.5
L8	5.5	5.0	4.0	18.0	16.5	21.1	62.7	61.9	48.3

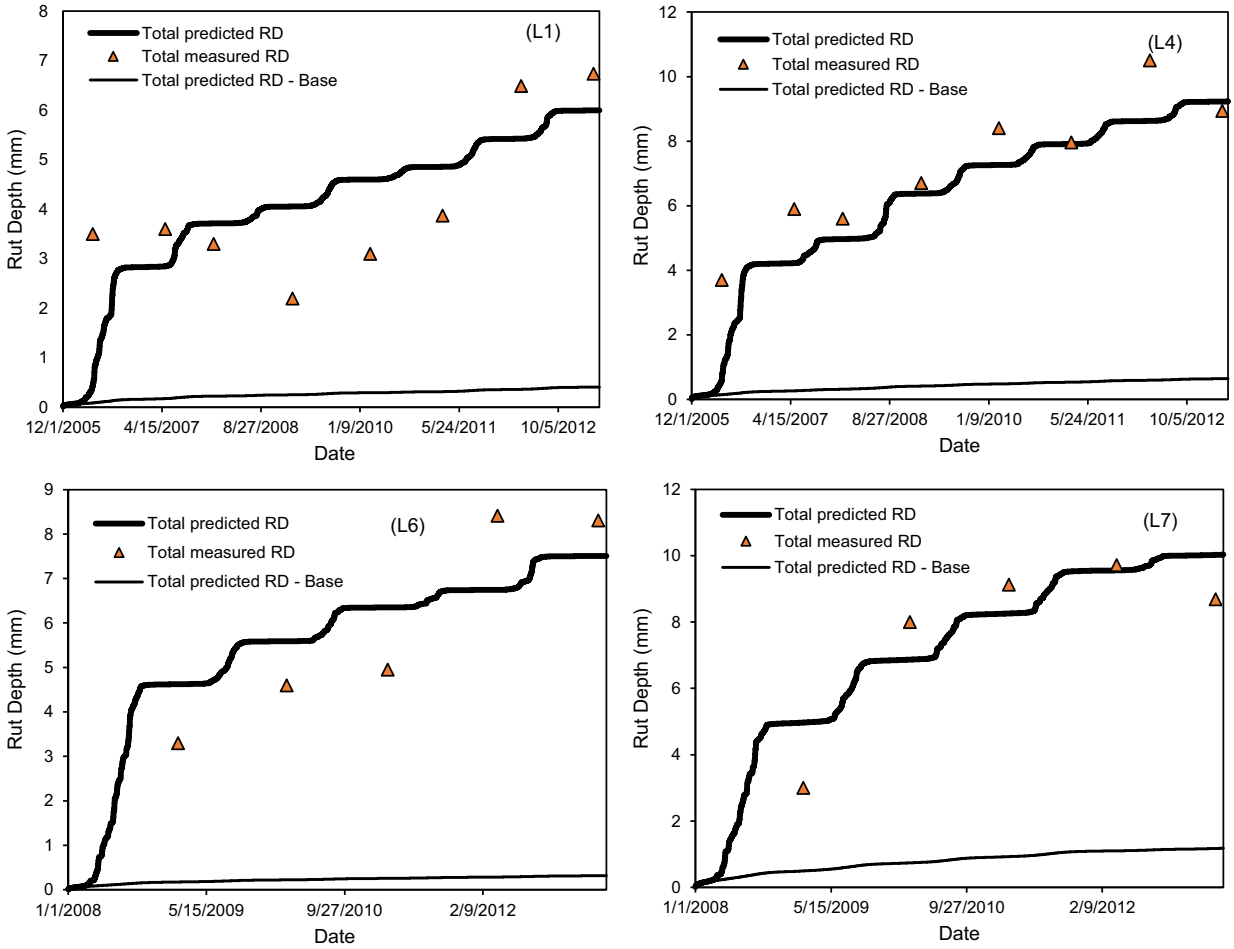

Fig. 11. Comparison between measured and computed rut depth versus time.

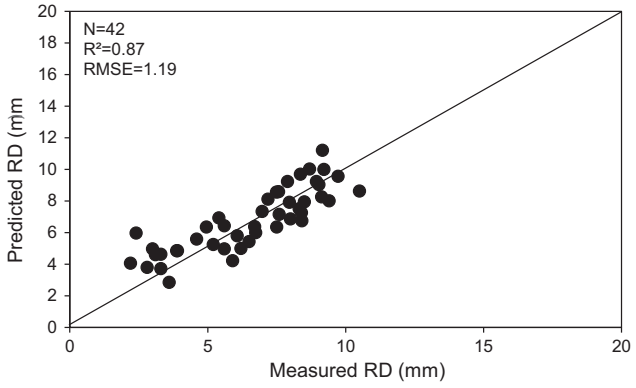

Fig. 12. Comparison between measured and computed rut depth for LTPP.

8. Conclusions

Prediction equations for shear properties of asphalt mixes, cohesion c and friction angle ϕ, were proposed in this study. Authors' original rutting model of asphalt mixes based on shear stress to strength ratio was revised, calibrated and validated. Some of the important findings in this study are summarized as follows:

- The shear strength, which is a function of c and ϕ, is an essential parameter representing resisting force of the AC to the rutting. Using laboratory test results of c and ϕ for various asphalt mixes, a multiple regression analyses were conducted to develop c and ϕ predictive equations at a reference temperature of 50 °C considering physical properties of asphalt binder and aggregate and volumetric properties of asphalt mixes. The prediction equations have a correlation coefficient of 0.87 and 0.86 for c and ϕ, respectively.
- A rutting model of asphalt mixes in a power law form was developed considering number of load cycles N, shear stress to strength ratio $\frac{\tau}{\tau_f}$, temperature T, and load duration t as main parameters contributing to permanent strain. The model coefficients were maintained constant regardless of mixture types and loading conditions.
- The rutting model was calibrated using field rutting data obtained from 26 pavement sections in WesTrack. It was further validated using LTPP data obtained from national highways in Korea. It was observed from the validation study that the rutting model proposed in this study successfully predicted rutting behavior of asphalt pavements. The predicted and measured rut depths were compared and the correlation coefficient and RMSE were 0.87 and 1.19 mm, respectively.

Acknowledgements

The authors would like to acknowledge partial support by Sejong University, BK21, Seoul Metropolitan Government and research project (Development of Eco-Friendly Pavements to Minimize Greenhouse Gas Emissions) funded by the Ministry of Land, Infrastructure and Transport(MOLIT) and the Korea Agency for Infrastructure Technology Advancement(KAIA).

References

[1] C.W. Schwartz, K.E. Kaloush, Permanent deformation assessment for asphalt concrete pavement and mixture design, in: Y.R. Kim (Ed.), Modeling of Asphalt Concrete, New York, McGraw-Hill Construction, 2009, pp. 317–351.

[2] A.C. Collop, A. Scarpas, C. Kasbergen, A. De Bondt, Development and Finite Element Implementation of Stress-Dependent Elastoviscoplastic Constitutive Model with Damage for Asphalt, J. Transport. Res. Board 2003 (1832) 96–104.

[3] N.H. Gibson, C.W. Schwartz, R.A. Schapery, M.W. Witczak, Viscoelastic, viscoplastic, and damage modeling of asphalt concrete in unconfined compression, J. Transport. Res. Board 2003 (1860) 3–15.

[4] Y.R. Kim, H.J. Lee, D.N. Little, Fatigue characterization of asphalt concrete using viscoelasticity and continuum damage theory, J. Assoc. Asphalt Paving Technol. 66 (1997) 520–569.

[5] H.J. Lee, Y.R. Kim, Viscoelastic constitutive model for asphalt concrete under cyclic loading, J. Eng. Mech. (ASCE) 124 (1998) 32–40.

[6] H.J. Lee, Y.R. Kim, Viscoelastic constitutive model for asphalt concrete with healing, J. Eng. Mech. (ASCE) 124 (1998) 1224–1232.

[7] G.R. Chehab, Y.R. Kim, M.W. Witczak, R. Bonaquist, Prediction of thermal Cracking Behavior of Asphalt Concrete using the Viscoelastoplastic Continuum Damage Model, 83rd Annual Meeting of the Transportation Research Board. Washinton D.C., 2004.

[8] W.J. Kenis, Predictive Design Procedures: A Design Methods for Flexible Pavement using the VESYS Structural Subsystem, in: Proceedings, 4th International Conference on the Structural Design of Asphalt Pavement. 1 (1997) 101–130.

[9] W.J. Kenis, W. Wang, Calibrating Mechanistic Flexible Pavement Rutting Models from Full Scale Accelerated Tests, Proceedings, 8th International Conference on the Structural Design of Asphalt Pavement. 1 (1997) 663–672.

[10] R.W. May, M.W. Witczak, An automated asphalt concrete mix analysis system, Proc. Assoc. Asphalt 61 (1992) 154–160.

[11] G. Baladi, Fatigue life and permanent deformation characteristics of asphalt concrete mixes, J. Transport. Res. Board 1227 (1989) 75–87.

[12] R.B. Leahy, Permanent Deformation Characteristics of Asphalt Concrete (Ph.D. Dissertation), University of Maryland, College Park, MD, 1989.

[13] M. Ayres, Development of a Rational Probabilisric Approach for Flexible Pavement Analysis (Ph.D. Dissertation), University of Maryland, College Park, MD, 1997.

[14] K.E. Kaloush, Simple Performance Test for Permanent Deformation of Asphalt Mixtures (Ph.D. Dissertation), Arizona State University, Temple, Ariz, 2001.

[15] NCHRP, Mechanistic-Empirical Design of New and Rehabilitated Pavement Structures, NCHRP Project 1–37A Draft Final Report, Transportation Research Board, Washington, D.C., 2004.

[16] Y.C. Suh, N.H. Cho, S. Mun, Development of mechanistic–empirical design method for an asphalt pavement rutting model using APT, Constr. Build. Mater. 25 (2011) 1685–1690.

[17] A.R. Archilla, L. de Lannoy Kobayashi, L.G. Diaz, Using permanent deformation tests and the MEPDG to quantify permanent deformation improvements from modified binders, J. Assoc. Asphalt Pavement Technol. 77 (2008) 1005–1035.

[18] C.L. Monismith, R.G. Hicks, F.N. Finn, J. Sousa, J. Harvey, S. Weissman, J. Deacon, J. Coplantz, G. Paulsen, Permanent Deformation Response of Asphalt Aggregate Mixes, Report no. SHRP-A-415, Strategic Highway Research Program, National Research Council, Washington, D.C., 1994.

[19] T.F. Fwa, S.A. Tan, L.Y. Zhu, Rutting prediction of asphalt pavement layer using c–ϕ Model, Journal of Transportation Engineering (ASCE). 675 (2004) 675–683.

[20] K. Su, L. Sun, Y. Hachiya, A new method for predicting rutting in asphalt pavements employing static uniaxial penetration test, Int. J. Pavement Res. Technol. 1 (2008) 24–33.

[21] Q. Li, H.J. Lee, E.Y. Hwang, Characterization of permanent deformation of asphalt mixtures based on shear properties, Journal of the Transportation Research Board. 2181 (2010) 45–52.

[22] Q. Li, H.J. Lee, S.Y. Lee, Permanent deformation model based on shear properties of asphalt mixtures development and calibration, J. Transport. Res. Board 2210 (2011) 81–89.

[23] NCHRP 455, Recommended Performance-Related Specification for Hot-Mix Asphalt Construction Results of the WesTrack Project, Transportation Research Board of the National Academies, Washington, DC, 2002.

[24] D.W. Christensen, R. Bonaquist, Use of strength for evaluating the rut resistance of asphalt concrete, J. Assoc. Asphalt Paving Technol. 71 (2002) 692–711.

[25] J. Zhu, L. Sun, L. Wang, H. Li, L. Liu, Development and calibration of shear-based rutting model for asphalt concrete layers, Int. J. Pavement Eng. 1080 (2016) 1–8.

[26] D.W. Christensen Jr., T.K. Pellinen, R.F. Bonaquist, Hirsch model for estimating the modulus of asphalt concrete, J. Assoc. Asphalt Paving Technol. 72 (2003) 692–711.

[27] V.P. Le, H.J. Lee, J.M. Flores, J. Baek, H.M. Park, Development of a simple asphalt concrete overlay design scheme based on mechanistic–empirical approach, Road Mater. Pavement Design 18 (2016) 630–645.

[28] S. Baltzer, J.M. Jansen, Temperature Correction of Asphalt-Moduli for FWD-Measurements, Proc., 4th Int. Conf. on Bearing Capacity of Roads and Airfields. 1 (1994), 753–763-768.

[29] E.O. Lukanen, R.N. Stubstad, R. Briggs, Temperature Predictions and Adjustment Factors for Asphalt Pavement, Report No. FHWA-RD-98-085. FHWA, Department of Transportaion, US, 2000.

[30] Harvey et al., Permanent Deformation Assessment for Asphalt Concrete Pavement and Mixture Design, in: Y.R. Kim (Ed.), Modeling of Asphalt Concrete, New York, McGraw-Hill construction, 2009, pp. 269–315.

[31] V.P. Le, H.J. Lee, J.M. Flores, W.J. Kim, J. Baek, New approach to construct master curve of damaged asphalt concrete based on falling weigh deflectometer back-calculated moduli, J. Transport. Eng. (ASCE) 142 (2016) 1–9.